Identification of the Ligands of Protein Interaction Domains through a Functional Approach*[S]

Ginevra Caratù‡§, Danilo Allegra‡§, Marida Bimonte‡, Gabriele Giacomo Schiattarella‡, Chiara D'Ambrosio¶, Andrea Scaloni¶, Maria Napolitano‖, Tommaso Russo‡, and Nicola Zambrano‡

The identification of protein-protein interaction networks has often given important information about the functions of specific proteins and on the cross-talk among metabolic and regulatory pathways. The availability of entire genome sequences has rendered feasible the systematic screening of collections of proteins, often of unknown function, aimed to find the cognate ligands. Once identified by genetic and/or biochemical approaches, the interaction between two proteins should be validated in the physiologic environment. Herein we describe an experimental strategy to screen collections of protein-protein interaction domains to find and validate candidate interactors. The approach is based on the assumption that the overexpression in cultured cells of protein-protein interaction domains, isolated from the context of the whole protein, could titrate the endogenous ligand and, in turn, exert a dominant negative effect. The identification of the ligand could provide us with a tool to check the relevance of the interaction because the contemporary overexpression of the isolated domain and of its ligand could rescue the dominant negative phenotype. We explored this approach by analyzing the possible dominant negative effects on the cell cycle progression of a collection of phosphotyrosine binding (PTB) domains of human proteins. Of 47 PTB domains, we found that the overexpression of 10 of them significantly interfered with the cell cycle progression of NIH3T3 cells. Four of them were used as baits to identify the cognate interactors. Among these proteins, CARM1, interacting with the PTB domain of RabGAP1, and EF1α, interacting with RGS12, were able to rescue the block of the cell cycle induced by the isolated PTB domain of the partner protein, thus confirming *in vivo* the relevance of the interaction. These results suggest that the described approach can be used for the systematic screening of the ligands of various protein-protein interaction domains also by using different biological assays. ***Molecular & Cellular Proteomics 6:333–345, 2007.***

From the ‡CEINGE Biotecnologie Avanzate, Dipartimento di Biochimica e Biotecnologie Mediche, Università di Napoli Federico II and ‖Istituto Nazionale dei Tumori "Fondazione Pascale," 80131 Napoli, Italy and ¶Proteomics and Mass Spectrometry Laboratory, ISPAAM, Consiglio Nazionale delle Ricerche, 80147 Napoli, Italy

Received, August 3, 2006, and in revised form, November 8, 2006
Published, MCP Papers in Press, November 23, 2006, DOI 10.1074/mcp.M600289-MCP200

The identification of novel protein-protein interactions has become a common strategy to assess the function of gene products. Taking into account the availability of biological sequence data and the annotations of genes in several species, systematic approaches have been realized in model organisms, from yeast to human, to define the molecular frames of binary interactions among proteins, which can be used to define the interactome of a given species (for a review, see Ref. 1). Identification of protein-protein interactions has taken advantage, in the last 2 decades, of both genetic and biochemical traps. Since its introduction, yeast two-hybrid screening (2) has served as a potent genetic tool to trap molecular interactions among proteins; its suitability to high throughput performance has been the result of its fundamental relevance to interactome mapping projects in invertebrates (3) as well as in mammalian species including human (4).

Besides genetic screens, alternative approaches are needed to overcome the limitations of the yeast systems. For instance, not all post-translational modifications relevant to some protein-protein interactions may properly occur in yeast cells (*i.e.* tyrosine phosphorylation). Furthermore the use of molecular baits encoding protein domains particularly small and/or prone to complex with other proteins, such as transcription activation domains, may in some cases preclude the feasibility of a genetic screen because of the high background. In this context, identification of biochemical interactions among proteins through co-precipitation assays provides a valid alternative approach to a detailed characterization of interactomes. This may be useful to find interactors for small protein binding motifs, which can be easily synthesized and derivatized for effective coupling to activated resins, or take advantage of recombinant expression of appropriate biochemical baits in bacteria or in eukaryotic cells. Once again, the availability of detailed annotations of biological sequences has accelerated the accumulation of data defining novel protein-protein interactions, also benefited by the availability of protein tagging strategies and the increased sensitivity of mass spectrometry-based methodologies for protein identification (5, 6). In any event, downstream of the capture of novel protein-protein interactions by either genetic or biochemical traps, molecular (co-fractionation and co-immunoprecipitation) and/or cellular (confocal microscopy and fluorescence resonance energy transfer analysis) approaches are required to confirm the occurrence of the complexes in living cells, and functional as-

says are necessary to assess their physiological relevance in the appropriate cellular context.

Adaptor proteins are specialized products, assembled through evolution-driven sequence modification and combinatorial shuffling of protein-protein interaction domains. For instance, SH2[1] and PTB domains from selected adaptors link activation of receptor tyrosine kinases to downstream signaling events regulating cellular proliferation, differentiation, and survival (7). Molecular adaptors are indeed involved in scaffolding the protein complexes necessary to perform and integrate distinct signaling pathways. Indeed the modular structures of adaptor proteins allow them to form complexes with one or more proteins at the same time. In turn, the bound proteins may link the former complexes to other proteins and, finally, to effector proteins. For these reasons, the expression of a protein domain, isolated from the context of the complete adaptor molecule, can render ineffective the progression of this molecular flow of interactions, preventing the formation of the ordered and functional protein complexes required for the effectiveness of the pathway. Thus, the overexpression of an isolated protein-protein interaction domain can be used as a functional tool to perturb cellular processes through dominant negative mechanisms. In this study, we describe a strategy aimed to identify and validate protein complexes based on the functional assay of the interaction. We decided to explore the interactions involving the phosphotyrosine binding domains (PTB or PID (phosphotyrosine interaction domain); for a review, see Ref. 8) present in a collection of human proteins. Despite the acronym, which would define this domain as a selective ligand for phosphotyrosine (Tyr(P)) residues, PTB domains are heterogeneous in their binding specificities: although IRS- and Shc-based PTB modules actually interact with phosphotyrosines, PTB domains from other proteins, such as Fe65, do not require the Tyr(P) residue for complex formation (9). Also in the absence of Tyr(P), which can be substituted for by unmodified tyrosine or by phenylalanine, the binding often requires a hydrophobic residue at -5, Asn at -3, and the Pro at -2. However, in several interactors of PTB domains it was impossible to find sequences with these characteristics, thus indicating pronounced heterogeneity in binding specificities (8). Given their participation in important cellular mechanisms, the proteins containing PTB domains often do participate in pathogenic mechanisms, such as in the case of oncogenic transformation (Shc) (10), hypercholesterolemia (ARH) (11), diabetes (IRS-1) (12), and developmental disorders (Dab) (13).

Considering the involvement of PTB domain-containing proteins in several signal transduction mechanisms, we speculated that at least some of these proteins could be involved in the regulation of cell cycle. Therefore, we have examined the possibility that isolated protein domains could act as dominant negative effectors, thus interfering with the progression of the cell cycle. According to this approach, we examined 47 PTB domains and found that the overexpression of 10 of them perturbed the cell cycle regulation. The ligands of four of these proteins were identified. Two of these ligands, CARM1, interacting with the PTB domain of RabGAP1, and EF1α, interacting with RGS12, were able to rescue the block of the cell cycle induced by the PTB domain of the partner protein, thus validating *in vivo* the relevance of the interaction.

EXPERIMENTAL PROCEDURES

In Silico Isolation of PTB Domains, Molecular Methods, and Library Setup—To obtain a full list of human PTB domains, we searched the Conserved Domains Section of the National Center for Biotechnology Information (NCBI) and the Ensembl databases; for the search in the latter database we considered both the annotated gene list (ENSG) and the protein family list (ENSF). The PTB domains were isolated from the full protein sequence using InterPro (14). The PTB domains showing a positive hit to one or more structural prediction programs were included; furthermore the PTB domains of EPS8L3 and CTEN, which were not detected by our approach, were also included, given their homology to the EPS8 family paralogs for EPS8L3 (15) and to the Tensin family members for CTEN (16).

The 47 human PTB domains were aligned with ClustalX (17) to determine the boundaries of the PTB domains; such information was used to design specific primers for RT-PCR amplification of the cDNA regions containing the domains. Total RNA preparations were obtained with the use of the RNeasy Mini kit (Qiagen) by three different human cell lines: human embryonic kidney HEK293 cells, IMR-90 fibroblasts, and SHSY-5Y neuroblastoma cells. The cDNAs for amplification were obtained through reverse transcription with Superscript II reverse transcriptase (Invitrogen) from DNase-treated RNA preparations using either oligo(dT) or random hexamers for priming. The individual PTB domain cDNAs were obtained by at least one of the three cell lines (for the sequences of the primers see Supplemental Table sd2) and cloned in the pEGFP-C1 vector (Invitrogen) in-frame to the EGFP coding region. The amplified cDNAs of the PTB domains were also cloned into a modified version of the pGEX2TK vector in which a sequence encoding the Strep-tag sequence WSHPQFEK was inserted 3′ to the vector polylinker. The cloning of the cDNAs allowed the expression of recombinant PTB domain polypeptides with an N-terminal GST tag and a C-terminal Strep-tag.

Cloning of the full-length cDNAs was achieved through RT-PCR amplification of EPS8L3, RabGAP1, RGS12, Q7Z2X4/P-CLI1, NMD3, and CARM1 cDNAs from at least one of the above cited human cell lines; the cDNAs for EF1α1 and the expression vector for LRP1 were a gift from Prof. P. Arcari and Prof. Strickland, respectively. The cDNAs for the PTB domain-containing proteins EPS8L3, RabGAP1, RGS12, and Q7Z2X4/P-CLI1 were cloned in-frame to a Myc tag, whereas the cDNAs of the ligands were cloned in-frame to the FLAG sequence, in the pRcCMV vector (Invitrogen). Supplemental Table sd3 reports the sequences of the oligonucleotides used for these amplifications.

Cell Cultures and Cell Cycle Analysis—NIH3T3, HEK293, IMR-90, and SHSY-5Y cells were grown in Dulbecco's modified Eagle's medium (Invitrogen) supplemented with 10% fetal bovine serum (Hyclone) using standard procedures. For metabolic labeling, NIH3T3 cultures were starved of methionine and cysteine for 30 min and then incubated in Dulbecco's modified Eagle's medium containing 0.08 mCi/ml [^{35}S]Met and [^{35}S]Cys mixture (Promix, GE Healthcare) for

[1] The abbreviations used are: SH, Src homology; PTB, phosphotyrosine binding; IRS, insulin receptor substrate; EF1α, elongation factor 1α; GAP, GTPase-activating protein; EPS, epidermal growth factor receptor protein substrate; BrdUrd, 5′-bromo-2′-deoxyuridine; LDL, low density lipoprotein; LRP1, LDL receptor-related protein 1; GFP, green fluorescent protein; EGFP, enhanced green fluorescent protein; HEK, human embryonic kidney; FACS, fluorescence-assisted cell sorting; JNK, c-Jun N-terminal kinase; RGS, regulators of G protein signaling; E13.5, embryonic day 13.5; SNARE, soluble *N*-ethylmaleimide-sensitive factor attachment protein receptors.

12 h before preparation of protein extracts. Cells were transfected with Lipofectamine 2000 (Invitrogen) according to the manufacturer's instructions. For fluorescence-assisted cell sorting (FACS) analysis, mouse fibroblasts NIH3T3 were plated in 60-mm dishes, allowed to attach to the dish overnight, and transiently transfected with the appropriate plasmids (10 μg of total DNA) using Lipofectamine 2000 (Invitrogen). Thirty hours after transfection, cells were dissociated from the plates with trypsin and washed with PBS without $CaCl_2$ and $MgCl_2$. Cells were then washed twice and fixed in 70% ethanol in PBS. Following another wash in the PBS, cells were treated with 10 μg/ml RNase A and then stained with 25 μg/ml propidium iodide. Transfected cells (20,000 cells for each experiment) were selected for analysis of DNA content (as measured by monitoring fluorescence from propidium iodide) by gating on fluorescein isothiocyanate-positive cells due to EGFP using a FACScan (BD Pharmingen). Cell cycle analysis was performed by the CELL-FIT program (BD Pharmingen). Three independent experiments were performed in triplicate. Statistical analysis was carried out with the Student's *t* test. For 5-bromo-2′-deoxyuridine (BrdUrd) incorporation experiments, NIH3T3 cells were grown on polylysine-precoated glass coverslips in 60-mm dishes and transfected with the appropriate vectors (10 μg of DNA) by using Lipofectamine 2000 (Invitrogen) according to the instructions from the manufacturer. Thirty hours after transfection, cells were incubated with 10 μM 5-bromo-2′-deoxyuridine (Roche Applied Science) for 2 h. Cells on coverslips were fixed with paraformaldehyde (4% in PBS, pH 7.4), permeabilized with 0.3% Triton X-100, and incubated with anti-BrdUrd monoclonal antibody (5-bromo-2′-deoxyuridine labeling and detection kit, Roche Applied Science) following the instructions of the supplier; then the cells were stained with Texas Red-conjugated secondary antibody (Jackson ImmunoResearch Laboratories). The coverslips were mounted in Mowiol (Calbiochem) onto a glass microscope slide, and fluorescence was examined using an Axiophot microscope (Zeiss). BrdUrd incorporation experiments were repeated three times for each transfected construct. In each independent experiment, BrdUrd-positive cells were scored from at least 200 EGFP-positive and 200 EGFP-negative cells. The ratios from the independent experiments were averaged, and standard deviation was calculated and reported on the chart.

Protein Expression and Purification, Mass Spectrometry, and Immunological Methods—The recombinant PTB domains from the modified pGEX2TK vector were expressed in the BL21 strain of *Escherichia coli* following induction of exponentially growing cultures with 0.25 mM isopropyl 1-thio-β-D-galactopyranoside for 3 h at room temperature. Recombinant proteins were extracted and purified on GSH-Sepharose following described procedures (9) and further purified on Streptactin-Sepharose columns. Final eluates, obtained with 2.5 mM desthiobiotin in 100 mM Tris-HCl, 150 mM NaCl, 1 mM EDTA, pH 8.00, were dialyzed against PBS containing 1 mM DTT and stored at −80 °C until use.

Cellular and embryo extracts were obtained by lysis in a buffer containing 50 mM Tris-HCl, 150 mM NaCl, 0,5% Triton X-100, 10% glycerol, pH 7.5, 50 mM NaF, 1 mM Na_3VO_4, 1 mM DTT, 0,4 mM EDTA, pH 8.0, and a mixture of protease inhibitors (Complete, Roche Applied Science). Lysates were clarified by centrifugation at 12,000 × *g* for 20 min at 4 °C. For radioactive pulldown, 250 μg of radiolabeled extracts from NIH3T3 cells were added to 10 μg of each recombinant protein bound to 10 μl of GSH-Sepharose resin; binding reactions were allowed to proceed for 2 h at 4 °C followed by washes in lysis buffer, elution, and loading onto 9% polyacrylamide gels for SDS-PAGE. Detection of bound proteins was obtained by scanning the fixed and dried gels on a Typhoon 9400 phosphorimaging system with the ImageQuant software (GE Healthcare).

Preparative pulldown experiments were performed with 10 nmol of the recombinant proteins bound to 100 μl of GSH-Sepharose. The embryo lysates (25 mg) were first run on a GST column for preclearing, then added to the recombinant proteins, and incubated for 2 h at 4 °C. The unbound proteins were removed by five washes in lysis buffer, and then the bound polypeptides were eluted by lysis buffer containing 1 M NaCl or by 2% SDS in Tris-HCl, pH 6.8. Alternatively after washes, the resin containing the bound material was exposed to thrombin protease (3 units) for 12 h at room temperature to release the PTB domains and the bound proteins. The collected material was separated by SDS-PAGE on 9% polyacrylamide gels, which were stained with silver nitrate according to standard procedures. Bands from SDS-PAGE were excised from the gel, minced, and washed with water. Proteins were in-gel reduced, *S*-alkylated, and digested with trypsin as reported previously (18). Digest aliquots were removed and subjected to a desalting/concentration step on C_{18} ZipTips (Millipore Corp., Bedford, MA) using acetonitrile as eluent before MALDI-TOF-MS analysis.

Peptide mixtures were loaded on the MALDI target, using the dried droplet technique and α-cyano-4-hydroxycinnamic acid as matrix, and analyzed by using a Voyager-DE PRO mass spectrometer (Applied Biosystems, Framingham, MA). Internal mass calibration was performed with peptides derived from enzyme autoproteolysis. The PROWL software package was used to identify bands unambiguously from the updated mammalian NCBI non-redundant sequence database (19). Candidates with ProFound estimated Z scores >1.8 were further evaluated by the comparison with their calculated mass using the experimental values obtained from SDS-PAGE. Detailed peptide mass fingerprint analysis is reported in the supplemental data.

Validation of the interactions was performed by pulldown followed by Western blot with antibodies directed against the endogenous or FLAG-tagged interactors of PTB domains: anti-CARM1 T-16 goat polyclonal (Santa Cruz Biotechnology); anti-eEF1α, CBP-KK1 mouse monoclonal (Upstate); anti-LRP1, rabbit polyclonal 483 (a kind gift from Dr. J. Herz); anti-FLAG peptide M2, mouse monoclonal (Sigma). Co-immunoprecipitations were carried out with the following antibody pairs: anti-FLAG M2 as precipitating antibody for NMD3-FLAG, CARM1-FLAG; anti-Myc 9E10 mouse monoclonal (Santa Cruz Biotechnology) as precipitating antibody for RGS12-Myc; anti-cubilin A-20 goat polyclonal (Santa Cruz Biotechnology). Detection of immune complexes in Western blot was carried out with the following antibodies: anti-Myc 9E10 for EPS8L3-Myc, RabGAP-Myc and Q7Z2X4; anti-eEF1α CBP-KK1. Detection for Western blot was carried out with the chemiluminescence system LiteAblot from Euroclone using horseradish peroxidase-conjugated protein A (GE Healthcare).

RESULTS AND DISCUSSION

Setup of a Library of PTB Domains—To build a collection of PTB domains, we searched GenBank™ and Ensembl databases to select the genes encoding proteins with this module. Considering the high level of conservation among the PTB domains of mammalian species, we focused on the human dataset, also assuming the presence of a higher number of entries and a more detailed annotation for human genes. To reduce the redundancy of information arising from GenBank and to avoid duplications from the combination of the outputs from the two databases, we aligned the 47 domains with ClustalW (20). We removed from analysis the proteins possessing an IRS-like PTB domain (8), which is annotated as a distinct entry in public databases (InterPro domain IPR002404). Our analysis was then focused on the remaining domains, classified as InterPro domain IPR006020, comprising both Shc-like and Dab-like PTBs (8). This approach led to

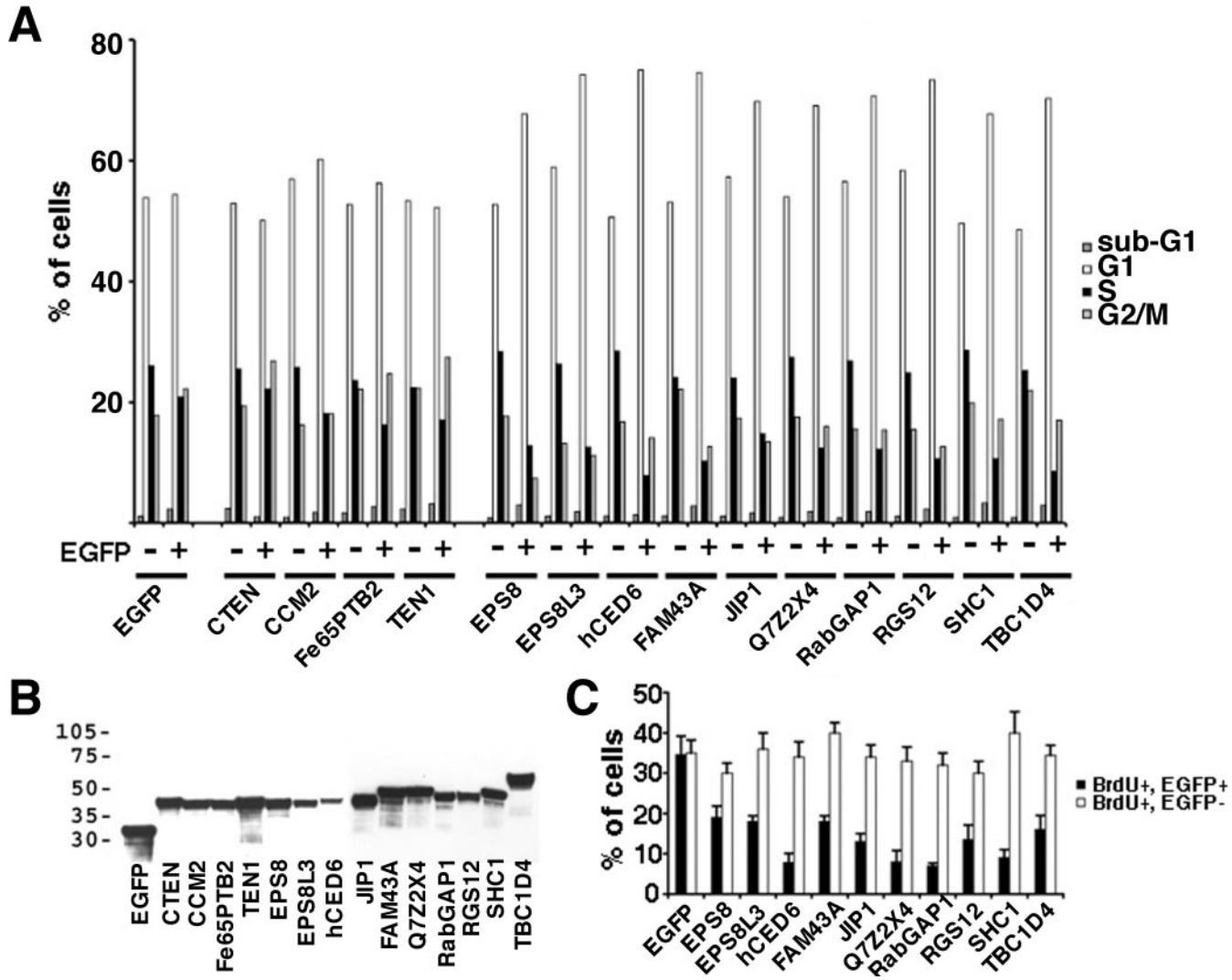

FIG. 1. **Overexpression of isolated PTB domains affects cell cycle progression in NIH3T3 cells.** *A*, cell cycle analysis of NIH3T3 cells transfected with the indicated EGFP-PTB constructs. After transfection, the cells were fixed, stained with propidium iodide, and analyzed by FACS. The results refer to the percentage of the cells with sub-G_1, G_1, S, and G_2/M DNA content in representative experiments in which cells from each transfection were sorted as EGFP-positive (transfected) and EGFP-negative (untransfected) populations. *B*, analysis of the expression of the PTB domains fused to EGFP by Western blot. The constructs of the indicated proteins were transfected in NIH3T3 cells. The fusion proteins were visualized with an EGFP monoclonal antibody. *C*, evaluation of DNA synthesis in cells transfected with the EGFP-PTB constructs by BrdUrd incorporation experiments. NIH3T3 cells transfected with the indicated EGFP-PTB constructs were labeled with BrdUrd, fixed and stained with 4′,6-diamidino-2-phenylindole to identify nuclei and with anti-BrdUrd monoclonal antibody to detect the cells in S phase. The BrdUrd-positive nuclei were counted by microscopic analysis in both transfected (*EGFP*+) and untransfected (*EGFP*−) populations. The chart reports the percent values of BrdUrd-positive cells in both populations. The standard deviation of triplicate experiments is reported.

the identification of 42 human genes coding for products with PTB domains. Considering that some proteins, such as Fe65 family members, do possess two PTB domains, the total number of our *in silico* search gave rise to 47 PTB modules. These are listed in Supplemental Table sd1; the table also indicates the known ligands for the PTB domains of previously characterized proteins.

A Subset of PTB Domains Perturbs Cell Cycle Progression in Mouse Fibroblasts—To examine the possible dominant effect of the overexpression of isolated PTB domains on the cell cycle progression, we generated the collection of PTB domains in the pEGFP-N eukaryotic expression vector, which allowed us to express the PTB domains with an N-terminal EGFP tag. Following the transfection of the constructs in NIH3T3 cells, we analyzed the distribution of transfected (GFP-positive) and untransfected (GFP-negative) cells in the G_0/G_1, S, and G_2/M phases of cell cycle by FACS analysis; the percentage of apoptotic cells (sub-G_1) was also established. In the first instance, the cells expressing the EGFP protein alone did distribute in a fashion highly superimposed to the non-GFP-expressing cells from all the tested constructs, indicating no side effects from GFP expression. In both cases,

the content of sub-G_1 cells ranged between 1.5 and 3.5% of total cells, so we set 5% as an arbitrary threshold for exclusion of potentially toxic PTB domains. Fig. 1*A* shows a representative set of data obtained with those PTB domains, inducing significant perturbations of the cell cycle, as well as the cell cycle distribution of cells transfected with the unmodified EGFP vector or with some constructs that did not alter significantly the cell cycle. We observed that the common effect of 10 overexpressed PTB domains was the increase of the number of cells in the G_1 phase of cell cycle accompanied by significant decrease of the S phase or of both S and G_2/M pools. This behavior suggests that the overexpressed domains mostly induce a G_1 arrest. Accordingly the estimation of proliferating cells by BrdUrd incorporation confirmed that the 10 GFP-PTB domains eliciting G_1 arrest show reduced proliferation because the number of cells involved in active DNA synthesis is decreased compared with the cells transfected with EGFP alone or with untransfected cells (Fig. 1*C*).

To understand the molecular basis of the events underlying the G_1 arrest, we designed a strategy to purify and identify the interactors of PTB domains through affinity chromatography with GST fusion proteins. To this aim, we transferred the collection of the PTB domains in a modified prokaryotic expression vector. The pGEX2TK plasmid, which normally allows the fusion of polypeptides to the N-terminal tag of GST, was improved by cloning the Strep-tag (21) to the C terminus of the recombinant proteins. This strategy allowed us to obtain highly purified biochemical baits of the PTB domains, devoid of contaminating *E. coli* proteins, for use as affinity matrices. The ability of the highly purified, correctly folded, and soluble PTB domains to work properly in protein-protein interaction assay was tested through co-precipitation with ^{35}S-labeled proteins from metabolically labeled NIH3T3 fibroblasts. Fig. 2 shows the results of some of the pulldown experiments, showing that the PTB domains specifically bind to labeled polypeptides.

Among the subset of PTB domains possessing the ability to interfere with cell cycle progression, we found some well characterized proteins, in terms of functional relevance and binding properties, such as Shc1, EPS8, hCed6, and JIP1. Given the involvement of Shc1 and EPS8 in the downstream events of receptor tyrosine kinase activation, it is expected that their isolated PTB domains may perturb mitogenic signaling and cell cycle progression. An additional member of the EPS8 family, EPS8L3, also possesses a PTB domain able to interfere, in a more pronounced way compared with EPS8, with cell cycle events. The JIP1 protein is another well described adaptor protein, binding to components of the JNK signaling module, involved in JNK activation (22).

hCed6/hGULP is the mammalian orthologue of the *Caenorhabditis elegans* gene *ced-6* (23). In the worm, it participates in the engulfment of apoptotic cells, acting as an adaptor for the phagocytic receptor, *CED-1*, through an interaction between the *CED-6* PTB domain and the NPLY motif in

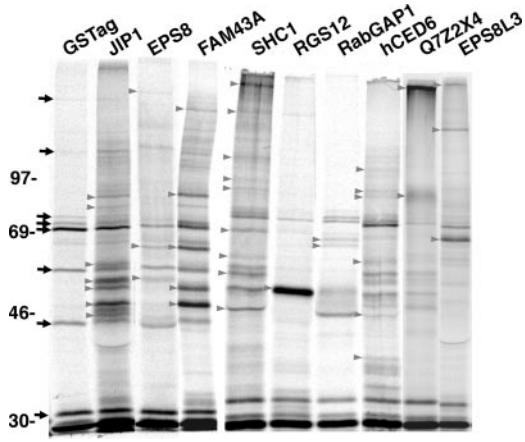

FIG. 2. **Interaction of PTB domains with cellular proteins.** The recombinant, bacterially expressed PTB domains fused to GST and Strep-tag were incubated with protein lysates from [^{35}S]Met and [^{35}S]Cys metabolically labeled NIH3T3 cells. The bound proteins were resolved by SDS-PAGE analysis and visualized with a phosphorimaging system. The *black arrows* indicate the proteins retained by the GST-Strep-tag (*GSTag*) control protein; the *gray arrowheads* indicate the proteins specifically retained by the PTB domains of the indicated proteins. Size markers are reported on the *left*.

CED-1. The involvement of hCed6 in apoptosis has been suggested by the ability of the human protein to partially rescue the engulfment defects of *ced-6* mutant worms (23).

hCed6 has also been shown to interact with the LDL receptor-like protein, LRP1, in an interaction enhanced by phosphorylation of the receptor (24). As expected from the known properties of all the previous proteins to serve as molecular scaffolds in relevant signal transduction mechanisms, several labeled proteins bind their PTB domains as confirmed by the pull-down experiment with radiolabeled proteins.

EPS8L3, RabGAP1, RGS12, and TBC1D4 are less characterized proteins compared with the previous proteins. RabGAP1 and TBC1D4 belong to a discrete group of proteins characterized by the TBC (Tre-2/Bub2/Cdc16)/Rab GTPase-activating protein homology domain (InterPro domain IPR000195), typical to proteins with GTPase-activating properties directed toward the Rab family of small G proteins. Due to the homology of RabGAP1 with the yeast spindle checkpoint protein Bub2p (25), its involvement in cell cycle events may be relevant. RGS12 also possesses a GAP activity domain, typical to the large family of regulators of G protein signaling (RGS) proteins; however, RGS12 has the unique property, among the various members of the family, to possess a PTB domain and a GoLoco motif (26). Finally only bioinformatic predictions are available for FAM43A and the annotated gene ENSG153823, encoding for the Q7Z2X4 protein.

Although the PTB domain of FAM43A binds to numerous labeled proteins, a more limited spectrum of interactors was observed with the PTB domains of RabGAP1, RGS12, and Q7Z2X4 proteins (see Fig. 2). Considering the absence of

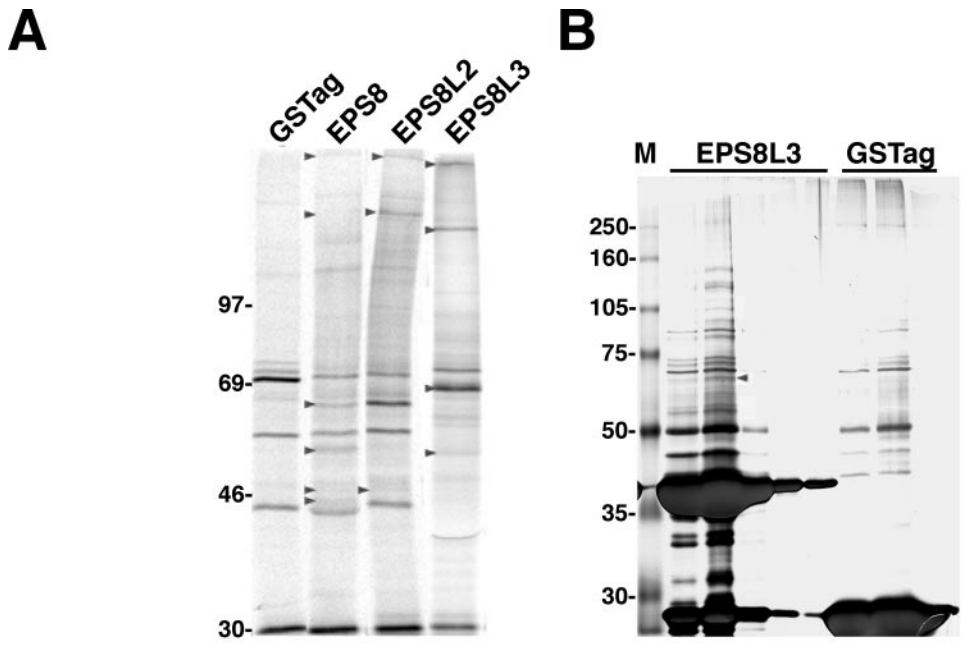

C

Band	Protein name	SwissProt code	Gene name	ProFound Est'd Z score	Peptides	Sequence coverage (%)	Mr	pI
1	NMD3 homolog	Q99L48	NMD3	2.22	10	24	57,611	6.78

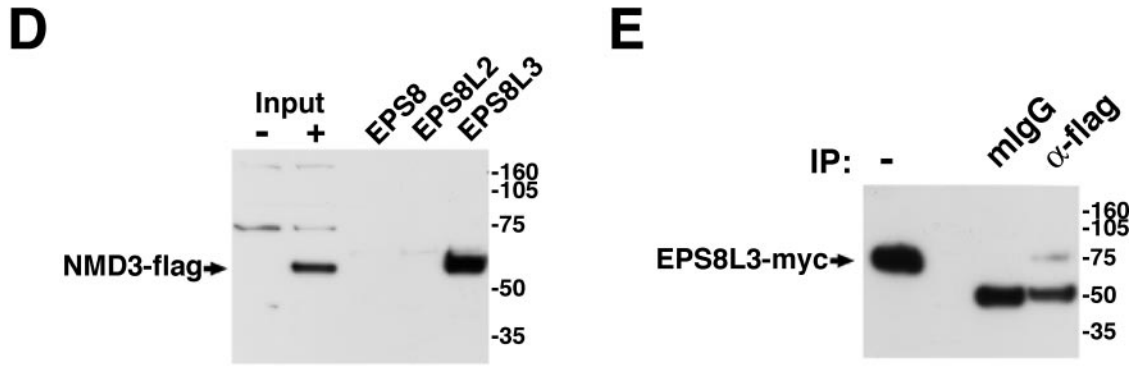

FIG. 3. **The NMD3 protein is a ligand of the EPS8L3 PTB domain.** *A*, the recombinant, bacterially expressed PTB domains fused to GST and Strep-tag were incubated with protein lysates from [^{35}S]Met and [^{35}S]Cys metabolically labeled NIH3T3 cells. The bound proteins were resolved by SDS-PAGE analysis and visualized with a phosphorimaging system. The *arrowheads* indicate the specific ligands. *Lane M*, molecular weight markers. *B*, the recombinant GST-Strep-tag (*GSTag*) and GST-EPS8L3 PTB proteins were incubated with E13.5 mouse embryo extracts. The bound proteins were resolved by SDS-PAGE analysis and visualized by silver staining. *C*, the protein band (*arrowhead* of *B*) was excised and subjected to proteolysis for mass spectrometry identification. The table shows the identification of the polypeptide as the mouse homolog of the human NMD3 protein. *D*, validation of the EPS8L3-PTB/NMD3 interaction by co-precipitation analysis. The recombinant PTB domains of EPS8, EPS8L2 and EPS8L3 fused to GST-Strep-tag were expressed in *E. coli* and incubated with extracts from NIH3T3 cells transfected with the full-length NMD3 cDNA fused to the FLAG epitope. The bound proteins were analyzed by Western blot with anti-FLAG antibody. The *arrow* indicates the migration of the NMD3-FLAG protein. 20 μg of cellular extracts from untransfected (−) or transfected (+) cells were loaded in the *first two lanes*, respectively, as a migration control. *E*, the full-length proteins EPS8L3 and NMD3 form a stable complex in mammalian cells. NIH3T3 fibroblasts were transfected with the full-length cDNAs of NMD3 fused to the FLAG epitope and of EPS8L3 fused to the Myc epitope. Extracts from transfected cells were immunoprecipitated with mouse IgG or with anti-FLAG antibody, and the complexes were analyzed with the Myc antibody. The *arrow* indicates the migration of the EPS8L3-Myc protein. 50 μg of cellular extracts from transfected cells were loaded in the *first lane* as a migration control. *Est'd*, estimated; *mIgG*, mouse IgG; *IP*, immunoprecipitation.

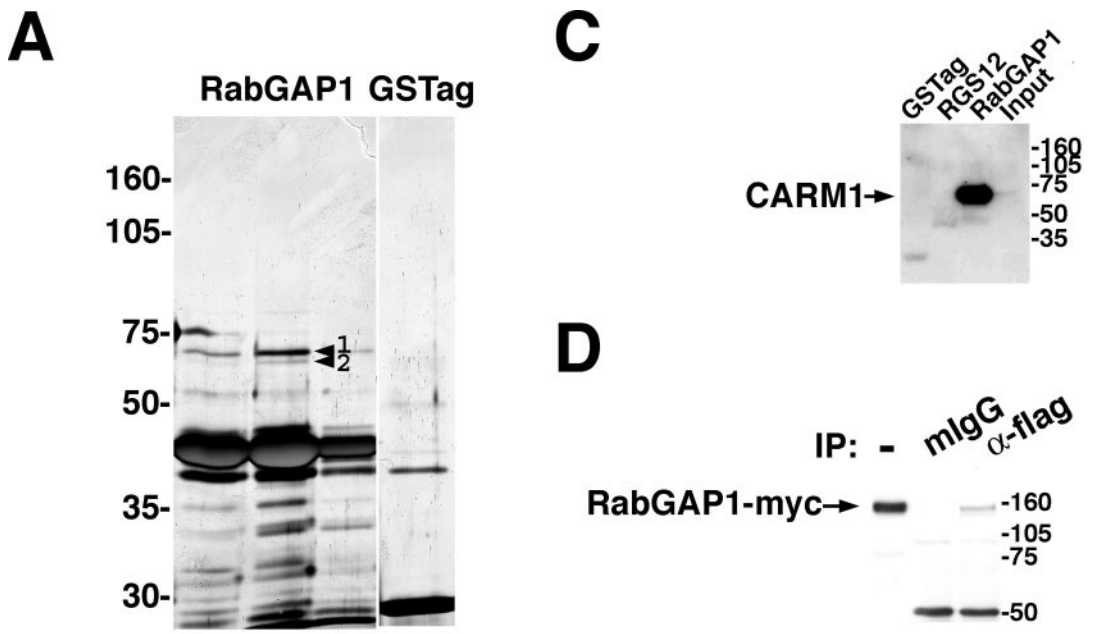

B

Band	Protein name	SwissProt code	Gene name	ProFound Est'd Z score	Peptides	Sequence coverage (%)	Mr	pI
1	Histone-arginine methyltransferase CARM1	Q9WVG6	CARM1	2.38	9	19	65,853	6.28
2	Histone-arginine methyltransferase CARM1	Q9WVG6	CARM1	1.89	6	16	65,853	6.28

FIG. 4. **The histone arginine methyltransferase CARM1 is a specific ligand of the RabGAP1 PTB domain.** *A*, rhe recombinant GST-Strep-tag (*GSTag*) and GST-RabGAP1 PTB proteins were incubated with E13.5 mouse embryo extracts. The bound proteins were resolved by SDS-PAGE analysis and visualized by silver staining. *B*, the protein *bands 1* and *2* (*arrowheads* of *A*) were excised and subjected to proteolysis for mass spectrometry identification. The table shows the identification of both polypeptides as the histone arginine methyltransferase CARM1. *C*, validation of the RabGAP1-PTB/CARM1 interaction by co-precipitation analysis. The recombinant GST-Strep-tag protein and the PTB domains of RGS12 and RabGAP1 fused to GST-Strep-tag were expressed in *E. coli* and incubated with extracts from E13.5 mouse embryos. The bound proteins were analyzed by Western blot with a CARM1 antibody. The *arrow* indicates the migration of the endogenous CARM1 protein. *D*, the full-length proteins RabGAP1 and CARM1 form a stable complex in mammalian cells. NIH3T3 fibroblasts were transfected with the full-length cDNAs of CARM1 fused to the FLAG epitope and of RabGAP1 fused to the Myc epitope. Extracts from transfected cells were immunoprecipitated with mouse IgG or with anti-FLAG antibody, and the complexes were analyzed with the Myc antibody. The *arrow* indicates the migration of the RabGAP1-Myc protein. 50 μg of cellular extracts from transfected cells were loaded in the *first lane* as a migration control. *Est'd*, estimated; *mIgG*, mouse IgG; *IP*, immunoprecipitation.

relevant information for the EPS8L3, RabGAP1, RGS12 and Q7Z2X4 proteins, we decided to use their PTB domains as baits for the identification of specific ligands.

Interactors of the EPS8-L3 PTB Domain—The proteins belonging to the EPS8 family show a conserved modular structure composed, N-terminal to C-terminal, of a PTB domain, an SH3 domain, and a C-terminal region (15). The most representative member of the family, EPS8, was discovered as a substrate for receptor tyrosine kinase activity of the epidermal growth factor receptor (27). The protein is involved in actin cytoskeleton dynamics and associated to membrane ruffle formation. Also the other members of the family, EPS8-L1 and -L2, bind actin and are more homologous to EPS8 than the EPS8-L3 protein (15). In our functional screening for modifiers of cell cycle progression, overexpression of both EPS8 and EPS8-L3 PTB domains is able to induce G_1 arrest; however, the latter is more efficient than EPS8. On the contrary, statistical analysis revealed that EPS8L2 did not induce significant perturbations of cell cycle (data not shown). Accordingly the pattern of proteins, which are bound by the PTB domains of the corresponding proteins, is different (Fig. 3*A*). In fact, although the three proteins tested share common ligands, spe-

cific interactors are displayed by both EPS8 and EPS8L3 but not by EPS8L2. To increase the complexity of the protein extracts, in terms of number of different proteins with the ability to interact with our PTB domains, we decided to use protein lysates from E13.5 mouse embryos. Fig. 3*B* shows the results of the preparative pulldown, which appeared particularly rich in potential interactors of the EPS8L3-PTB protein. However, MALDI-TOF identification of the putative ligands showed that several protein bands were due to aggregation of the protein bait. Among these polypeptides, we were able to identify the 65-kDa band, also present in the radiolabeled lysate, as the NMD3 protein (Fig. 3*C*). A pulldown experiment, shown in Fig. 3*D*, confirmed that NMD3 is an actual and specific interactor of EPS8L3 because the overexpressed, tagged NMD3 protein is specifically recognized by EPS8L3-PTB, and not by GST alone, or by the PTB domains of either EPS8 or EPS8L2. Furthermore the interaction occurs between the two full-length proteins because a specific complex is co-precipitated by Myc antibody in cells expressing the EPS8L3-Myc and the NMD3-FLAG proteins (Fig. 3*E*).

The PTB Domain of RabGAP1 Binds the Arginine Methyltransferase CARM1—As for the EPS8L3 PTB domain, the RabGAP1 PTB domain acts as a strong inducer of G_1 arrest in NIH3T3 cells. Its PTB domain, fused to GST, has been used in preparative pulldown experiments with protein extracts from mouse embryos. The domain is able to bind specifically two closely migrating polypeptides with molecular masses of about 60 kDa (Fig. 4*A*) that have been identified by mass spectrometry fingerprint as the coactivator-associated Arg methyltransferase CARM1 (Fig. 4*B*). The validation of the interaction between the two proteins was achieved in the pulldown of the recombinant GST-RabGAP1 PTB domain with the endogenous CARM1 protein (Fig. 4*C*). To verify the presence of a complex between the full-length RabGAP1 and CARM1 proteins, we co-precipitated the complex between the two tagged proteins, expressed in NIH3T3 cells. The Western blot of Fig. 4*D* shows that the Myc-RabGAP1 protein is detected specifically in immune complexes containing the FLAG-CARM1 protein.

An RGS12·eEF1α Complex Assembles in Mammalian Cells—Similarly to RabGAP1, RGS12 is involved in the activation of GTPase activity of G proteins because of the presence, in its coding region, of an RGS domain. It is thus expected that RGS12 works as a regulator of the activity of G proteins. RGS12 is a unique member of the family of RGS proteins because it has a specific combination of protein-protein interaction domains (N-terminal PDZ and PTB domains) and the GoLoco domain (26), which is associated to guanine nucleotide dissociation inhibitor activity (28). It is then expected that RGS12 forms complexes with proteins involved in molecular events mediated by G proteins. We performed preparative pulldown experiments with the RGS12-PTB fusion protein; because the radioactive pulldown indicated the presence of a strong ligand migrating in a position (45 kDa) close to the recombinant protein, we subjected the material retained by the affinity matrix to digestion with the thrombin protease. In fact, a vector-encoded thrombin site is present in the fusion protein in the linker region between the GST and the PTB domain. The material loaded on the preparative gel showed the presence of a series of seven polypeptides (Fig. 5*A*), which were all identified as a unique protein, suggesting that the different fragments were derived by proteolytic digestion of the retained protein. Indeed mass spectrometry data indicated that the ligand of the RGS12-PTB protein was the translation elongation factor eEF1α1 (Fig. 5*B*). A recent report indicated that a region encompassing the RGS12 PTB domain interacts with the SNARE-binding region of the Cav2.2 calcium channel (29). This interaction requires the phosphorylation of a tyrosine in a sequence differing from the classical NP*X*Y motif recognized by other PTB domains. We were not able to identify such protein in our assay probably because of the limited amount of tyrosine-phosphorylated channel in the embryo extract. However, the interaction of RGS12-PTB with eEF1α1 is highly specific as demonstrated by the pulldown (Fig. 5*C*) and the co-precipitation of the Myc-tagged RGS12 (Fig. 5*D*) with the endogenous, native eEF1α1.

The Novel Protein Q7Z2X4 Interacts with Protein Complexes Formed by the LDL Receptor-related Protein LRP1—The gene ENSG153823 encodes for an *in silico* annotated product, corresponding to the Q7Z2X4 protein. The structure of this protein is very simple: a 250-amino acid-long peptide mainly composed of the PTB domain. Expressed sequence tag data, as well as our RT-PCR experiment, aiming to isolate the corresponding PTB domain for cloning, do confirm that the annotated gene is actually expressed. The purification of interactors for the PTB domain of Q7Z2X4 reveals proteins with a very high molecular mass; indeed proteins with an elevated molecular weight are specifically co-precipitated with the radiolabeled (Fig. 2) and with the cold lysates (Fig. 6*A*). Mass spectrometry-based fingerprint analysis identified two proteins, the LDL receptor-related protein, LRP1, and cubilin, as interactors of Q7Z2X4 PTB domain (Fig. 6*B*). LRP1 is a member of the LDL receptor-related proteins; it is derived from a precursor, which is cleaved and arranged as a heterodimer, possessing a large (515-kDa), extracellular domain, linked by disulfide bond to the small (85-kDa), membrane-spanning domain. Fig. 6*C* confirms the MS-based identification of LRP1 as a specific ligand of the Q7Z2X4 PTB domain. Cubilin is a large (460-kDa), peripheral membrane protein known to associate to megalin, another member of the LDL receptor-related protein family, and to the receptor-associated protein RAP, a 39-kDa protein that interacts with all the lipoprotein receptors in the endoplasmic reticulum (30). Given the absence of transmembrane and cytosolic domains in cubilin, its interaction with the PTB domain of Q7Z2X4 strongly suggests that the latter co-precipitates within a large complex involving both LRP1 and cubilin. Indeed co-immunoprecipitation with a cubilin antibody followed by Western

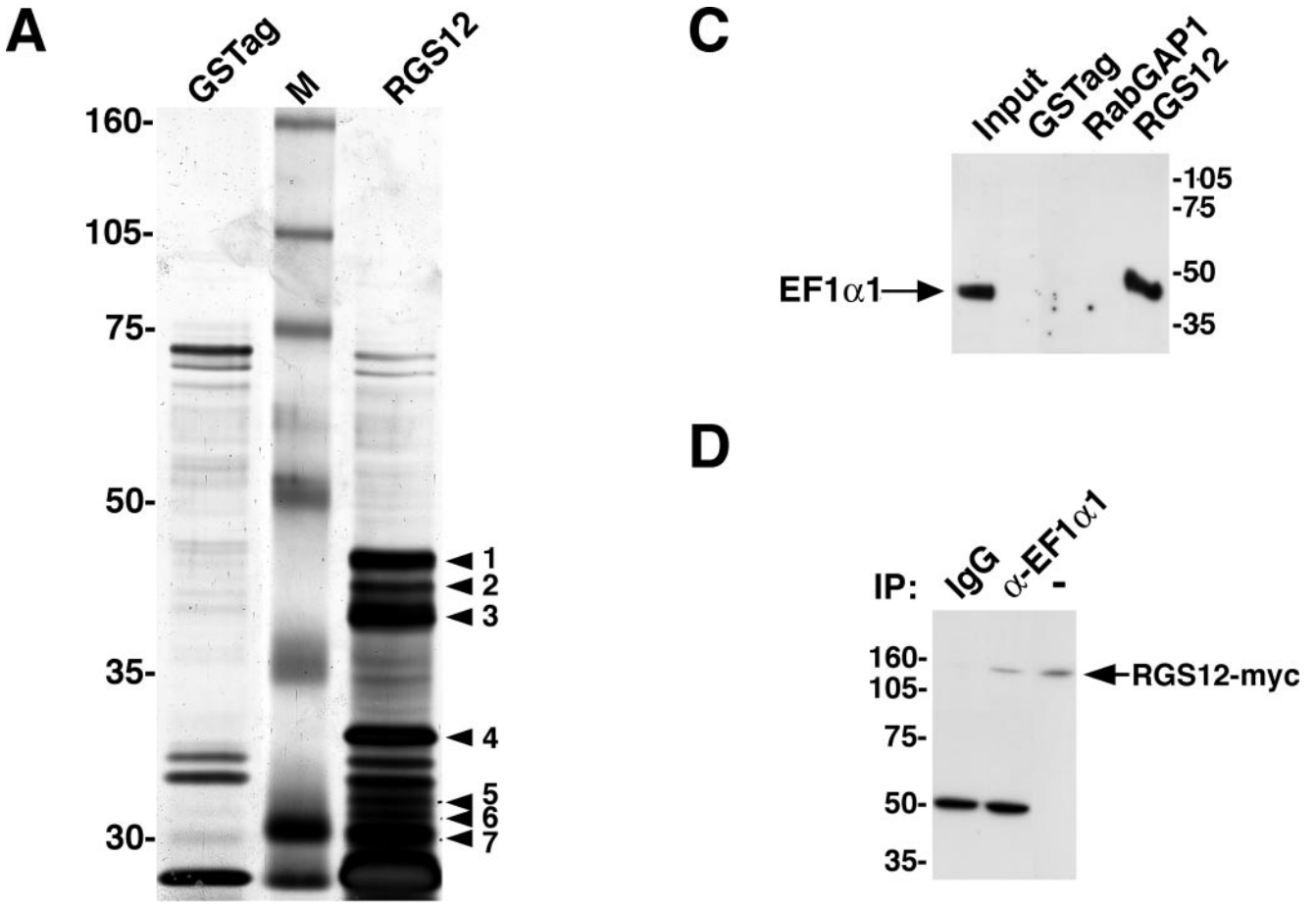

B

Band	Protein name	SwissProt code	Gene name	ProFound Est'd Z score	Peptides	Sequence coverage (%)	Mr	pI
1	Elongation factor 1-alpha 1	P10126	EEF1A1	2.00	7	24	50,113	9.10
2	Elongation factor 1-alpha 1	P10126	EEF1A1	2.31	8	35	50,113	9.10
3	Elongation factor 1-alpha 1	P10126	EEF1A1	2.26	8	29	50,113	9.10
4	Elongation factor 1-alpha 1	P10126	EEF1A1	2.40	14	41	50,113	9.10
5	Elongation factor 1-alpha 1	P10126	EEF1A1	2.01	9	32	50,113	9.10
6	Elongation factor 1-alpha 1	P10126	EEF1A1	2.01	8	29	50,113	9.10
7	Elongation factor 1-alpha 1	P10126	EEF1A1	2.15	9	28	50,113	9.10

FIG. 5. **The translation elongation factor EF1α1 is a specific ligand of the RGS12 PTB domain.** *A*, the recombinant GST-Strep-tag (*GSTag*) and GST-RGS12 PTB proteins were incubated with E13.5 mouse embryo extracts. The bound proteins were digested with thrombin protease, resolved by SDS-PAGE analysis, and visualized by silver staining. *Lane M*, molecular weight markers. *B*, the protein *bands 1–7* (*arrowheads* of *A*) were excised and subjected to proteolysis for mass spectrometry identification. The table shows the identification of the seven polypeptides as the elongation factor EF1α1. *C*, validation of the RGS12-PTB/EF1α1 interaction by co-precipitation analysis. The recombinant GST-Strep-tag protein and the PTB domains of RabGAP1 and RGS12 fused to GST-Strep-tag were expressed in *E. coli* and incubated with extracts from E13.5 mouse embryos. The bound proteins were analyzed by Western blot with the EF1α1 antibody. The *arrow* indicates the migration of the endogenous EF1α1 protein. 10 μg of extract were loaded in the *first lane* as a migration control. *D*, the full-length proteins RGS12 and EF1α1 form a stable complex in mammalian cells. NIH3T3 fibroblasts were transfected with the full-length cDNA of RGS12 fused to the Myc epitope. Extracts from transfected cells were immunoprecipitated with mouse IgG or with anti-EF1α1 antibody, and the complexes were analyzed with the Myc antibody. The *arrow* indicates the migration of the RGS12-Myc protein. 20 μg of cellular extracts from transfected cells were loaded in the *last lane* as a migration control. *Est'd*, estimated; *IP*, immunoprecipitation.

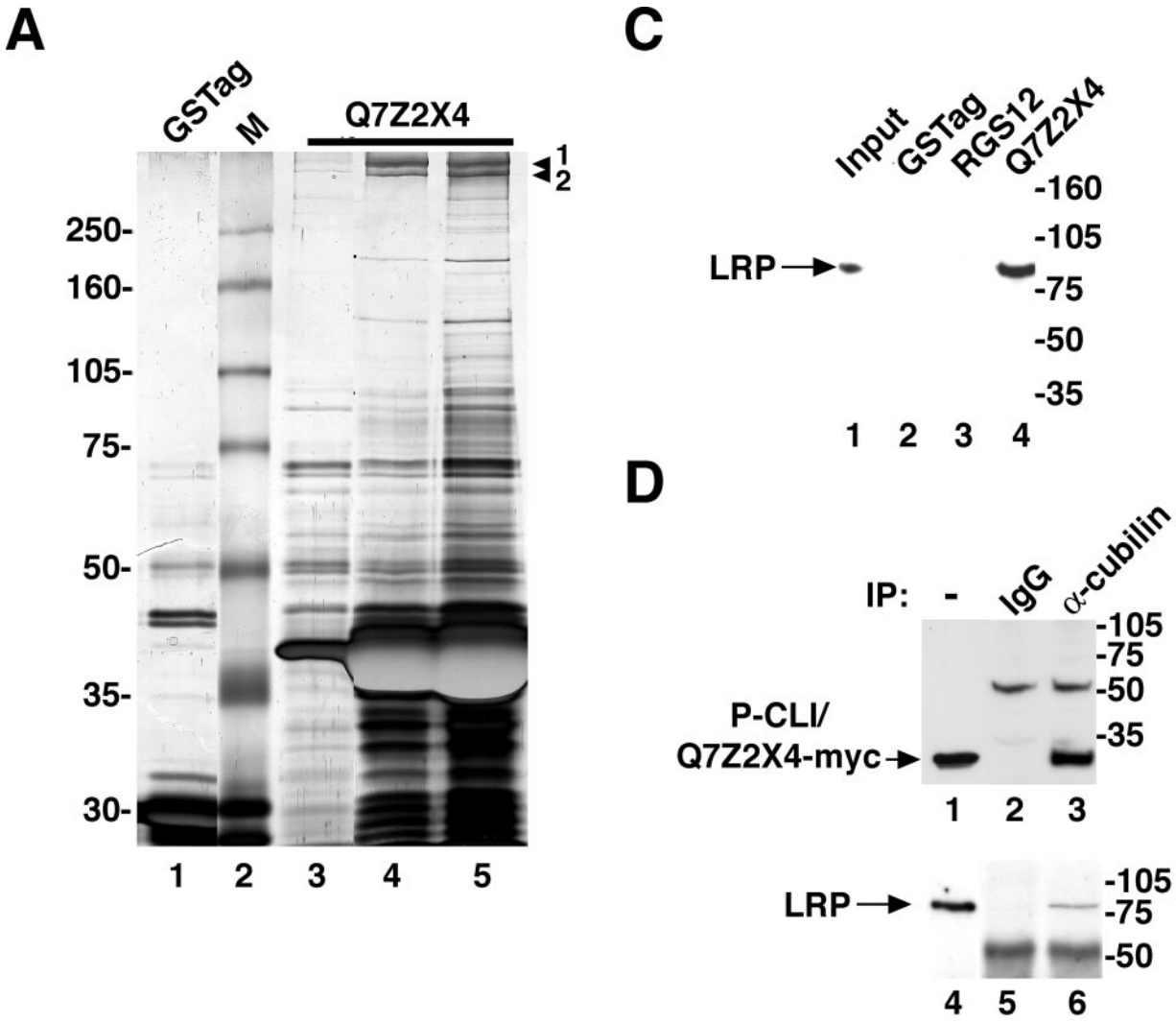

B

Band	Protein name	SwissProt code	Gene name	ProFound Est'd Z score	Peptides	Sequence coverage (%)	Mr	pI
1	Lipoprotein receptor-related protein	Q920Y4	LRP1	2.38	42	12	504,771	5.14
2	Cubilin	Q9JLB4	CUBN	2.35	16	8	395,498	5.43

FIG. 6. **The novel protein Q7Z2X4/P-CLI1 is part of a trimeric complex with the membrane proteins cubilin and LRP1.** *A*, the recombinant GST-Strep-tag (*GSTag*) and GST-Strep-tag-Q7Z2X4/PTB proteins were incubated with E13.5 mouse embryo extracts. The bound proteins were eluted with salts (1 M NaCl in lysis buffer) and collected in three fractions (*lanes 3–5*). The samples were resolved by SDS-PAGE analysis and visualized by silver staining. *Lane M*, molecular weight markers. *B*, the protein *bands 1* and *2* (*arrowheads* of *A*) were excised and subjected to proteolysis for mass spectrometry identification. The table shows the identification of the two polypeptides as the lipoprotein receptor-related protein LRP1 and cubilin, respectively. *C*, validation of the Q7Z2X4-PTB/LRP1 interaction by co-precipitation analysis. The recombinant GST-Strep-tag protein and the PTB domains of RGS12 and Q7Z2X4 fused to GST-Strep-tag were expressed in *E. coli* and incubated with extracts from E13.5 mouse embryos. The bound proteins were analyzed by Western blot with an LRP1 antibody. The *arrow* indicates the migration of the endogenous LRP1 protein. 10 μg of extract were loaded in the *first lane* as a migration control. *D*, cubilin forms stable complexes with Q7Z2X4 and LRP1 in mammalian cells. NIH3T3 fibroblasts were transfected with the full-length cDNA of Q7Z2X4 fused to the Myc epitope. Extracts from transfected cells were immunoprecipitated with control IgG or with a cubilin antibody, and the complexes were analyzed with the Myc antibody (*lanes 1–3*) or with the LRP1 antibody (*lanes 4–6*). The *arrows* indicate the migration of the Q7Z2X4/P-CLI1-Myc protein and LRP1 C-terminal domain, respectively. 50 μg of cellular extracts from transfected cells were loaded in the *first lanes* as migration controls. *Est'd*, estimated; *IP*, immunoprecipitation.

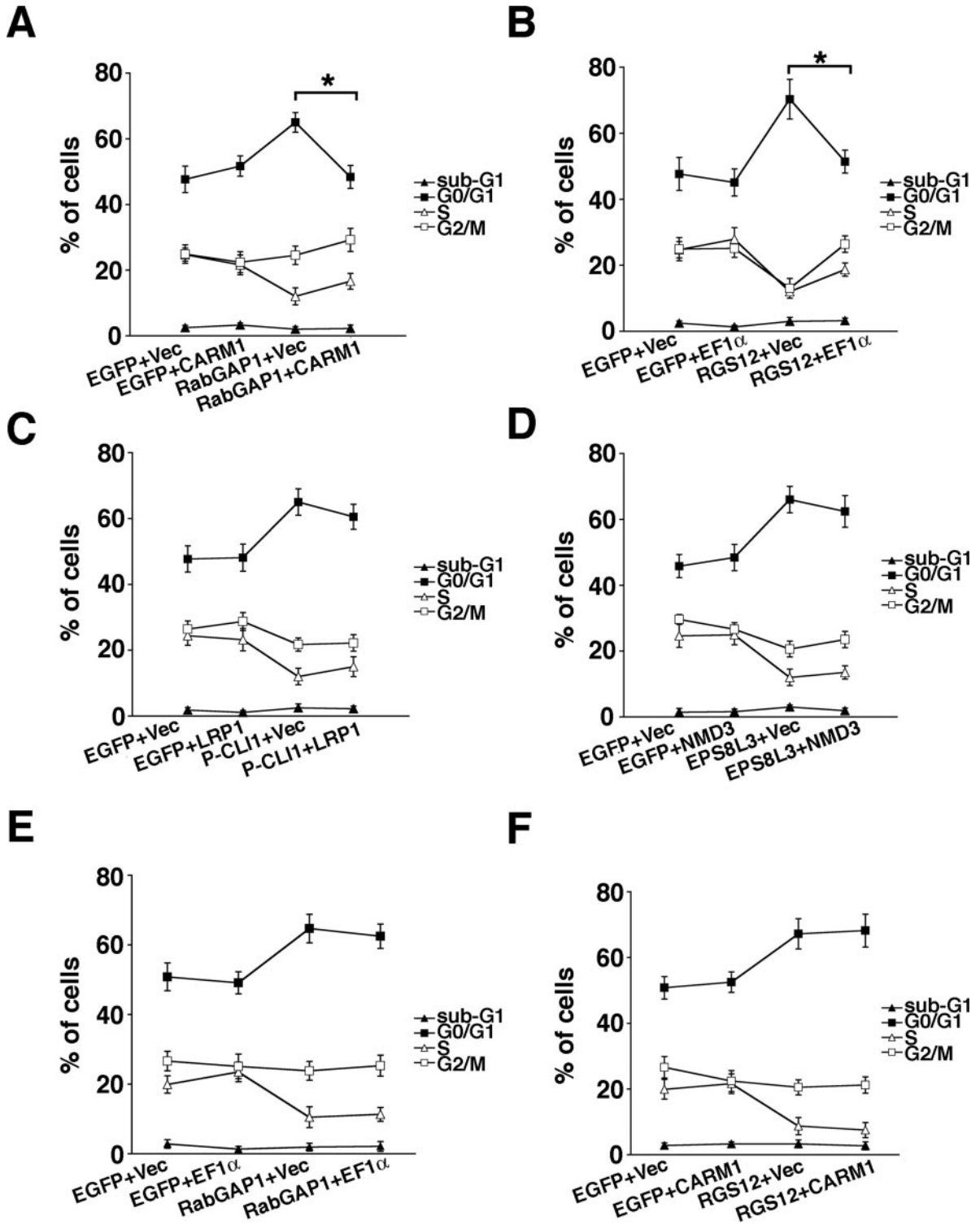

FIG. 7. **The G_1 arrest triggered by the isolated PTB domains of RabGAP1 and RGS12 is rescued by the overexpression of the cognate ligands CARM1 and EF1α1.** FACS analyses of NIH3T3 cells transfected with the PTB domains fused to EGFP of RabGAP1 (*A*), RGS12 (*B*), Q7Z2X4/P-CLI1 (*C*), and EPS8L3 (*D*) with the tagged, full-length interactors CARM1, EF1α1, LRP1, and NMD3, respectively, or with empty expression vectors is shown. In *E* and *F*, NIH3T3 cells were transfected with the RabGAP1-PTB domain fused to EGFP and EF1α1 or with the RGS12 PTB domain fused to EGFP and CARM1, respectively. The charts also report the cell cycle distributions of control cells transfected with EGFP alone or with EGFP and the vectors encoding the full-length CARM1, EF1α1, LRP1, and NMD3 proteins. After transfection, the cells were fixed, stained with propidium iodide, and analyzed by FACS. The results refer to EGFP-positive cells from three independent experiments. The *asterisks* in *A* and *B* indicate *p* values <0.001. *Vec*, vector.

blot with the Myc antibody to reveal the overexpressed Q7Z2X4 protein (*lanes 1–3*) or with LRP1 antibody to detect the endogenous protein (*lanes 4–6*) suggests the formation of the trimeric complex cubilin·LRP1·Q7Z2X4 (Fig. 6*D*). On the basis of this experimental evidence we suggest to assign to the Q7Z2X4 protein the name P-CLI1 (PTB-containing cubilin-LRP1-interacting protein).

Functional Rescue of G_1 Arrest by Overexpression of PTB Domain Ligands—The biochemical experiments carried out on the EPS8L3·NMD3, RabGAP1·CARM1, RGS12·EF1α1, and P-CLI1·LRP1·cubilin complexes demonstrated the physical association of these proteins in living cells. Taking into account the demonstrated ability of the isolated PTB domains to exert arrest of cell cycle progression, we tested the functional relevance of the novel complexes in cell cycle. Indeed we postulated that the simultaneous overexpression of the PTB modules and cognate interactors could generate a condition overwhelming the effects of the isolated domains and then leading to the functional rescue of the cell cycle progression arrest. We then set up experiments aiming to relieve the cells from G_1 arrest induced by the PTB domains of EPS8L3, RabGAP1, RGS12, and P-CLI1, co-transfect the cognate ligands, and analyze cell cycle distribution of transfected cells, through FACS analysis, as the readout. Transfection experiments were performed with amounts of the EGFP-PTB plasmids 3 times lower than those of the vectors expressing the interactor. This strategy allows us to assume that the interactors are expressed in most of the GFP-sorted cells.

We measured the percentage of cells in G_0/G_1, S, and G_2/M phases 36 h after the transfection of the EGFP-PTB constructs or the co-transfection of the EGFP-PTBs with the cognate interactors described above. As shown in Fig. 7*A*, CARM1 co-transfection almost completely abolished the G_1 arrest provoked by RabGAP1-PTB. The same significant effect was observed with EF1α1 in cells co-transfected with RSG12-PTB (see Fig. 7*B*). On the contrary, both LRP1 and NMD3 were unable to rescue the phenotype induced by P-CLI1 and EPS8L3, respectively (see Fig. 7, *C* and *D*).

The most plausible interpretation of these results is that the two pairs, P-CLI1·LRP1 and EPS8L3·NMD3, are not involved in the control of the cell cycle progression, and thus the effects observed in cells overexpressing the isolated PTB domains of P-CLI1 and EPS8L3 are due to the titration of other partners that we did not identify in the pulldown experiments. Another possibility is that the rescue was not successful because of an incorrect stoichiometry of the co-transfected proteins possibly due to the different expression levels of the vectors and/or of the turnover of the recombinant proteins.

On the contrary, in the first two cases the results suggest that we have identified the relevant *in vivo* ligands of RabGAP1 and RGS12, *i.e.* CARM1 and EF1α, respectively. This is also confirmed by the inability of CARM1 to overcome the G_1 arrest elicited by the PTB domain of RGS12; accordingly the overexpression of EF1α does not rescue the accumulation of the cells expressing the PTB domain of RabGAP1 in the G_1 phase of the cell cycle (Fig. 7, *E* and *F*). These results prove that the experimental strategy was working efficiently. On this basis, we think that it also can be extended to other collections of isolated protein-protein interaction domains whose possible dominant effects can be also analyzed in several biological assays, such as those measuring cell differentiation, regulation of apoptosis, cell migration, interference with signaling, etc.

* This work was supported in part by grants from the VI Framework Programme of the European Community-APOPIS Consortium, from the Alzheimer's Association, and from MIUR-PRIN 2005 (to N. Z. and T. R.). The costs of publication of this article were defrayed in part by the payment of page charges. This article must therefore be hereby marked "*advertisement*" in accordance with 18 U.S.C. Section 1734 solely to indicate this fact.

S The on-line version of this article (available at http://www.mcponline.org) contains supplemental material.

§ Both authors contributed equally to this work.

** To whom correspondence should be addressed: CEINGE Biotecnologie Avanzate, Via Comunale Margherita 482, 80145 Napoli, Italy. Tel.: 390813737877; Fax: 390813737808; E-mail: zambrano@dbbm.unina.it.

REFERENCES

1. Cusick, M. E., Klitgord, N., Vidal, M., and Hill, D. E. (2005) Interactome: gateway into systems biology. *Hum. Mol. Gen.* **14,** 171–181
2. Fields, S., and Song, O. (1989) A novel genetic system to detect protein-protein interactions. *Nature* **340,** 245–246
3. Li, S., Armstrong, C. M., Bertin, M., Ge, H., Milstein, S., Boxem, M., Vidalain, P. O., Han, J. D., Chesmeau, A., Hao, T., Goldberg, D. S., Li, N., Martinez, M., Rual, J. F., Lamesch, P., Xu, L., Tewari, M., Wong, S. L., Zhang, L. V., Berriz, G. F., Jacotot, L., Vaglio, P., Reboul, J., Hirozane-Kishikawa, T., Li, Q., Gabel, H. W., Elewa, A., Baumgartner, B., Rose, D. J., Yu, H., Bosak, S., Sequerra, R., Fraser, A., Mango, S. E., Saxton, W. M., Strome, S., Van Den Heuvel, S., Piano, F., Vandenhaute, J., Sardet, C., Gerstein, M., Doucette-Stamm, L., Gunsalus, K. C., Harper, J. W., Cusick, M. E., Roth, F. P., Hill, D. E., and Vidal, M. (2004) A map of the interactome network of the metazoan *C. elegans. Science* **303,** 540–543
4. Rual, J. F., Venkatesan, K., Hao, T., Hirozane-Kishikawa, T., Dricot, A., Li, N., Berriz, G. F., Gibbons, F. D., Dreze, M., Ayivi-Guedehoussou, N., Klitgord, N., Simon, C., Boxem, M., Milstein, S., Rosenberg, J., Goldberg, D. S., Zhang, L. V., Wong, S. L., Franklin, G., Li, S., Albala, J. S., Lim, J., Fraughton, C., Llamosas, E., Cevik, S., Bex, C., Lamesch, P., Sikorski, R. S., Vandenhaute, J., Zoghbi, H. Y., Smolyar, A., Bosak, S., Sequerra, R., Doucette-Stamm, L., Cusick, M. E., Hill, D. E., Roth, F. P., and Vidal, M. (2005) Towards a proteome-scale map of the human protein-protein interaction network. *Nature* **437,** 1173–1178
5. Gavin, A. C., Bosche, M., Krause, R., Grandi, P., Marzioch, M., Bauer, A., Schultz, J., Rick, J. M., Michon, A. M., Cruciat, C. M., Remor, M., Hofert, C., Schelder, M., Brajenovic, M., Ruffner, H., Merino, A., Klein, K., Hudak, M., Dickson, D., Rudi, T., Gnau, V., Bauch, A., Bastuck, S., Huhse, B., Leutwein, C., Heurtier, M. A., Copley, R. R., Edelmann, A., Querfurth, E., Rybin, V., Drewes, G., Raida, M., Bouwmeester, T., Bork, P., Seraphin, B., Kuster, B., Neubauer, G., and Superti-Furga, G. (2002) Functional organization of the yeast proteome by systematic analysis of protein complexes. *Nature* **415,** 141–147
6. Ho, Y., Gruhler, A., Heilbut, A., Bader, G. D., Moore, L., Adams, S. L., Millar, A., Taylor, P., Bennett, K., Boutilier, K., Yang, L., Wolting, C., Donaldson, I., Schandorff, S., Shewnarane, J., Vo, M., Taggart, J., Goudreault, M., Muskat, B., Alfarano, C., Dewar, D., Lin, Z., Michalickova, K., Willems, A. R., Sassi, H., Nielsen, P. A., Rasmussen, K. J., Andersen, J. R., Johansen, L. E., Hansen, L. H., Jespersen, H., Podtelejnikov, A., Nielsen,

E., Crawford, J., Poulsen, V., Sorensen, B. D., Matthiesen, J., Hendrickson, R. C., Gleeson, F., Pawson, T., Moran, M. F., Durocher, D., Mann, M., Hogue, C. W., Figeys, D., and Tyers, M. (2002) Systematic identification of protein complexes in *Saccharomyces cerevisiae* by mass spectrometry. *Nature* **415,** 180–183

7. Pawson, T. (2004) Specificity in signal transduction: from phosphotyrosine-SH2 domain interactions to complex cellular systems. *Cell* **116,** 191–203
8. Uhlik, M. T., Temple, B., Bencharit, S., Kimple, A. J., Siderovski, D. P., and Johnson, G. L. (2005) Structural and evolutionary division of phosphotyrosine binding (PTB) domains. *J. Mol. Biol.* **345,** 1–20
9. Zambrano, N., Buxbaum J. D., Minopoli, G., Fiore, F., De Candia, P., De Renzis, S., Faraonio, R., Sabo, S., Cheetham, J., Sudol, M., and Russo, T. (1997) Interaction of the phosphotyrosine interaction/phosphotyrosine binding-related domains of Fe65 with wild-type and mutant Alzheimer's β-amyloid precursor proteins. *J. Biol. Chem.* **272,** 6399–6405
10. Pelicci, G., Lanfrancone, L., Grignani, F., McGlade, J., Cavallo, F., Forni, G., Nicoletti, I., Grignani, F., Pawson, T., and Pelicci, P. G. (1992) A novel transforming protein (SHC) with an SH2 domain is implicated in mitogenic signal transduction. *Cell* **70,** 93–104
11. Garcia, C. K., Wilund, K., Arca, M., Zuliani, G., Fellin, R., Maioli, M., Calandra, S., Bertolini, S., Cossu, F., Grishin, N., Barnes, R., Cohen, J. C., and Hobbs, H. H. (2001) Autosomal recessive hypercholesterolemia caused by mutations in a putative LDL receptor adaptor protein. *Science* **292,** 1394–1398
12. Porzio, O., Federici, M., Hribal, M. L., Lauro, D., Accili, D., Lauro, R., Borboni, P., and Sesti, G. (1999) The Gly972→Arg amino acid polymorphism in IRS-1 impairs insulin secretion in pancreatic beta cells. *J. Clin. Investig.* **104,** 357–364
13. Sheldon, M., Rice, D. S., D'Arcangelo, G., Yoneshima, H., Nakajima, K., Mikoshiba, K., Howell, B. W., Cooper, J. A., Goldowitz, D., and Curran, T. (1997) Scrambler and yotari disrupt the disabled gene and produce a reeler-like phenotype in mice. *Nature* **389,** 730–733
14. Mulder, N. J., Apweiler, R., Attwood, T. K., Bairoch, A., Bateman, A., Binns, D., Bradley, P., Bork, P., Bucher, P., Cerutti, L., Copley, R., Courcelle, E., Das, U., Durbin, R., Fleischmann, W., Gough, J., Haft, D., Harte, N., Hulo, N., Kahn, D., Kanapin, A., Krestyaninova, M., Lonsdale, D., Lopez, R., Letunic, I., Madera, M., Maslen, J., McDowall, J., Mitchell, A., Nikolskaya, A. N., Orchard, S., Pagni, M., Ponting, C. P., Quevillon, E., Selengut, J., Sigrist, C. J., Silventoinen, V., Studholme, D. J., Vaughan, R., and Wu, C. H. (2005) InterPro, progress and status in 2005. *Nucleic Acids Res.* **33,** 201–205
15. Tocchetti, A., Confalonieri, S., Scita, G., Di Fiore, P.P., and Betsholtz, C. (2003) In silico analysis of the EPS8 gene family: genomic organization, expression profile, and protein structure. *Genomics* **81,** 234–244
16. Lo, S. H. (2004) Tensin. *Int. J. Biochem. Cell Biol.* **36,** 31–34
17. Jeanmougin, F., Thompson, J. D., Gouy, M., Higgins, D. G., and Gibson, T. J. (1998) Multiple sequence alignment with Clustal X. *Trends Biochem. Sci.* **23,** 403–405
18. D'Ambrosio, C., Arena, S., Fulcoli, G., Scheinfeld, M. H., Zhou, D., D'Adamio, L., and Scaloni, A. (2006) Hyperphosphorylation of JNK-interacting protein 1, a protein associated with Alzheimer disease. *Mol. Cell. Proteomics* **5,** 97–113
19. Zhang, W., and Chait, B. T. (2000) ProFound: an expert system for protein identification using mass spectrometric peptide mapping information. *Anal. Chem.* **72,** 2482–2489
20. Higgins, D., Thompson, J., Gibson, T., Thompson, J. D., Higgins, D. G., and Gibson, T. J. (1994) CLUSTAL W: improving the sensitivity of progressive multiple sequence alignment through sequence weighting position-specific gap penalties and weight matrix choice. *Nucleic Acids Res.* **22,** 4673–4680
21. Schmidt, T. G., Koepke, J., Frank, R., and Skerra, A. (1996) Molecular interaction between the Strep-tag affinity peptide and its cognate target, streptavidin. *J. Mol. Biol.* **255,** 753–766
22. Jaeschke, A., Czech, M. P., and Davis, R. J. (2004) An essential role of the JIP1 scaffold protein for JNK activation in adipose tissue. *Genes Dev.* **18,** 1976–1980
23. Mangahas, P. M., and Zhou, Z. (2005) Clearance of apoptotic cells in *Caenorhabditis elegans*. *Semin. Cell Dev. Biol.* **16,** 295–306
24. Ranganathan, S., Liu, C. X., Migliorini, M. M., Von Arnim, C. A., Peltan, I. D., Mikhailenko, I., Hyman, B. T., and Strickland, D. K. (2004) Serine and threonine phosphorylation of the low density lipoprotein receptor-related protein by protein kinase Cα regulates endocytosis and association with adaptor molecules. *J. Biol. Chem.* **279,** 40536–40544
25. Cuif, M. H., Possmayer, F., Zander, H., Bordes, N., Jollivet, F., Couedel-Courteille, A., Janoueix-Lerosey, I., Langsley, G., Bornens, M., and Goud, B. (1999) Characterization of GAPCenA, a GTPase activating protein for Rab6, part of which associates with the centrosome. *EMBO J.* **18,** 1772–1782
26. Ishii, M., and Kurachi, Y. (2003) Physiological actions of regulators of G-protein signaling (RGS) proteins. *Life Sci.* **74,** 163–171
27. Fazioli, F., Minichiello, L., Matoska, V., Castagnino, P., Miki, T., Wong, W. T., and Di Fiore, P. P. (1993) Eps8, a substrate for the epidermal growth factor receptor kinase, enhances EGF-dependent mitogenic signals. *EMBO J.* **12,** 3799–3808
28. Willard, F. S., Kimple, R. J., and Siderovski, D. P. (2004) Return of the GDI: the GoLoco motif in cell division. *Annu. Rev. Biochem.* **73,** 925–951
29. Richman, R. W., Strock, J., Hains, M. D., Cabanilla, N. J., Lau, K. K., Siderovski, D. P., and Diverse-Pierluissi, M. (2005) RGS12 interacts with the SNARE-binding region of the Cav2.2 calcium channel. *J. Biol. Chem.* **280,** 1521–1528
30. Christensen, E. I., and Birn, H. (2002) Megalin and cubilin: multifunctional endocytic receptors. *Nat. Rev. Mol. Cell. Biol.* **3,** 256–266